

# Interacting boson fermion-fermion model calculation of the $h_{11/2}h_{11/2}$ doublet bands in $^{134}\text{Pr}$

---

**Brant, Slobodan; Vretenar, Dario; Ventura, A.**

*Source / Izvornik:* **Physical Review C - Nuclear Physics, 2004, 69**

**Journal article, Published version**

**Rad u časopisu, Objavljena verzija rada (izdavačev PDF)**

<https://doi.org/10.1103/PhysRevC.69.017304>

*Permanent link / Trajna poveznica:* <https://um.nsk.hr/um:nbn:hr:217:831882>

*Rights / Prava:* [In copyright](#)/[Zaštićeno autorskim pravom.](#)

*Download date / Datum preuzimanja:* **2024-07-11**



*Repository / Repozitorij:*

[Repository of the Faculty of Science - University of Zagreb](#)



**Interacting boson fermion-fermion model calculation of the  $\pi h_{11/2} \otimes \nu h_{11/2}$  doublet bands in  $^{134}\text{Pr}$** 

S. Brant and D. Vretenar

*Department of Physics, Faculty of Science, University of Zagreb, Zagreb, Croatia*

A. Ventura

*Ente Nuove Tecnologie, Energia e Ambiente, Bologna, Italy  
and Istituto Nazionale di Fisica Nucleare, Sezione di Bologna, Italy*

(Received 4 July 2003; published 28 January 2004)

The interacting boson fermion-fermion model is employed in the analysis of the positive-parity doublet bands in  $^{134}\text{Pr}$ . It is shown that stable triaxial deformation gives rise to the experimentally observed crossing between the yrast and yrare bands built on the  $\pi h_{11/2} \otimes \nu h_{11/2}$  configuration. The collective structure of the yrast band is basically built on the ground-state band of the triaxial core, whereas the collective structure of the yrare band is predominantly based on the  $\gamma$  band of the core. The mixing between the two bands increases with angular momentum. A constant energy spacing between the two lowest positive-parity bands is predicted in other odd-odd  $N=75$  nuclei with  $\gamma$ -soft potential energy surfaces.

DOI: 10.1103/PhysRevC.69.017304

PACS number(s): 21.10.Re, 23.20.Lv, 23.90.+w, 27.60.+j

In their pioneering work [1] Frauendorf and Meng pointed out that the rotation of triaxial nuclei may give rise to pairs of identical  $\Delta I=1$  bands with the same parity in odd-odd nuclei—chiral doublet bands. These structures arise from configurations in which the angular momenta of the valence proton, the valence neutron, and the core are mutually perpendicular, and can be arranged to form two systems that differ by intrinsic chirality, a left- and a right-handed system. When chiral symmetry is thus broken in the body-fixed frame, the restoration of the symmetry in the laboratory frame results in the occurrence of degenerate doublet  $\Delta I=1$  bands. It has been suggested that such nearly degenerate rotational bands might be observed in the region of transitional nuclei with  $A \approx 130$ . A number of nuclei in this region are susceptible to triaxial deformation and the yrast bands of odd-odd nuclei are built on the  $\pi h_{11/2}$  particlelike- $\nu h_{11/2}$  holelike configuration. In Ref. [2] the existence of self-consistent rotating mean-field solutions with chiral character has been demonstrated for  $^{134}\text{Pr}$  and  $^{188}\text{Ir}$ . The theoretical prediction of chiral doublet structures has prompted quite a number of experimental studies of odd-odd  $N=75$  and  $N=73$  isotones in the  $A \approx 130$  region, and nearly degenerate  $\Delta I=1$  bands built on the  $\pi h_{11/2} \otimes \nu h_{11/2}$  configuration have been identified in many of these nuclei. In Ref. [3] in particular, new sideband partners of the  $\pi h_{11/2} \otimes \nu h_{11/2}$  yrast band have been identified in  $^{55}\text{Cs}$ ,  $^{57}\text{La}$ , and  $^{61}\text{Pm}$   $N=75$  isotones of  $^{134}\text{Pr}$ . For  $^{134}\text{Pr}$  the energy spacing between the doublet rotational bands gradually decreases from  $\approx 0.19$  MeV at low spin to the point where the two bands cross between  $I=14$  and  $I=15$ . For the other  $N=75$  isotones the two lowest  $\pi h_{11/2} \otimes \nu h_{11/2}$  bands are almost parallel in the  $E$  vs  $I$  plot, and the energy spacing between the corresponding states with the same spin is  $\approx 0.3$  MeV.

In  $^{134}\text{Pr}$  the two lowest, yrast, and yrare  $\pi h_{11/2} \otimes \nu h_{11/2}$  bands have been interpreted as chiral restored doublet bands [1–3]. In order to explain similar doublet bands in the other  $N=75$  odd-odd nuclei, it has been suggested that in these cases the triaxial core deformation is not stable, but perhaps more  $\gamma$  soft, resulting in collective chiral vibration of the core angular momentum between the left- and right-handed

chiral systems [3]. It has to be emphasized that in all studies of chiral doublet bands it has been argued that the empirical separation of  $\leq 300$  keV is too small for the sideband to be interpreted as a band built either on the unfavored signature of the proton orbital, or on the  $\gamma$ -vibrational excitation. A  $\gamma$ -vibration coupled to the yrast band has been ruled out [3] because in this region the  $\gamma$ -vibration energies are  $\geq 600$  keV.

In the present work we calculate the lowest bands in  $^{134}\text{Pr}$  in the framework of the interacting boson fermion-fermion model (IBFFM) [4,5]. Based on the highly successful interacting boson model (IBM-1) [6,7] for even-even nuclei, and the interacting boson-fermion model (IBFM) [8,9] for odd- $A$  nuclei, the IBFFM has been applied in the description of the structure of vibrational, deformed, and transitional odd-odd nuclei all over the periodic table. The IBM/IBFM approach to the structure of collective states in nuclei, based on the interacting boson approximation, is especially relevant for nuclei in transitional regions, where single-particle excitations and vibrational collectivity are dominant modes. In the IBM/IBFM framework calculations are performed in the laboratory frame and the results can be directly compared with experimental data. All states within the model space and their electromagnetic properties are compared with experiment, rather than just band-head energies.

The IBFFM [4,5] description of the positive-parity structures in  $^{134}\text{Pr}_{75}$  is fully consistent and starts with the calculation of its even-even and odd-even neighbors. The spectrum of positive-parity states in  $^{134}\text{Pr}$ , based on negative-parity orbitals of the odd proton and odd neutron, is calculated by using the quasiparticle energies, occupation probabilities, and boson-fermion interaction strengths obtained in the IBFM [8,9] calculations of negative-parity spectra in  $^{135}\text{Pr}_{76}$  and  $^{133}\text{Ce}_{75}$ . Most of the model parameters, therefore, are determined by the structure of collective and single-nucleon states in the even-even and odd-even neighbors of  $^{134}\text{Pr}$  and, in principle, only the residual interaction between the odd proton and odd neutron has to be adjusted to the experimental data in the odd-odd nucleus. In the following calculation the interaction strengths, effective charges,

and gyromagnetic ratios are defined according to Refs. [5,10].

The spectrum of the core nucleus  $^{134}_{58}\text{Ce}_{76}$  is described by the Hamiltonian

$$H_{IBM} = \epsilon_d \hat{n}_d + pP \cdot P + k'L \cdot L + kQ \cdot Q + \Theta_3 [(d^\dagger d^\dagger)_2 d^\dagger]_3 \cdot [(\tilde{d}\tilde{d})_2 \tilde{d}]_3. \quad (1)$$

The first four terms represent the standard Hamiltonian of the IBM-1 [6,7]. The cubic interaction in the last term, with the strength parameter  $\Theta_3$ , is included in order to introduce a degree of triaxiality [11,12]. The best agreement with the experimental spectrum is obtained for the following choice of parameters:  $\epsilon_d=0.75$ ,  $p=0.25$ ,  $k'=0.014$ ,  $k=-0.003$ ,  $\Theta_3=0.025$  (all in MeV), and  $\chi=-0.3$  in the quadrupole operator  $Q_2$ . This value of  $\chi$  is also used in the boson quadrupole operator appearing in the boson-fermion dynamical interaction, as well as in the  $E2$  operator. The number of  $s$  and  $d$  bosons is  $N=7$ . The same set of boson parameters is also used in the calculation of the two odd- $A$  nuclei and of  $^{134}\text{Pr}$ , except that a fine tuning of the triaxiality parameter to  $\Theta_3=0.03$  MeV improves the agreement of the positive-parity structures with the experimental spectrum of  $^{134}\text{Pr}$ . This fine tuning includes additional polarization effects of the odd proton and odd neutron on the triaxial core.

In Fig. 1 we compare the calculated low-energy spectrum of  $^{134}\text{Ce}$  with available experimental levels of the ground-state band, the  $\gamma$ -band, and some higher-lying structures. The levels in the left columns correspond to the IBM-1 calculation with  $\Theta_3=0$  in the Hamiltonian (1), i.e., the term that induces triaxial deformation is not included. The resulting spectrum is close to the  $O(6)$  limit of the IBM and is characteristic for a  $\gamma$ -soft nucleus. The calculated ground-state band is in reasonable agreement with the experimental sequence, but the  $\gamma$ -band displays the characteristic doublet structure not observed in the experimental spectrum. The middle columns present the ground-state band, the  $\gamma$ -band, and levels belonging to higher structures, calculated with  $\Theta_3=0.025$  MeV. The cubic term in the Hamiltonian induces a stable triaxial deformation and the agreement with the experimental spectrum is much improved. In particular, the inclusion of the three-body boson interaction lowers the odd-spin members of the  $\gamma$  band and therefore removes the quasidegenerate doublet structure, i.e., the odd-even staggering of the  $\gamma$  band is much less pronounced. In addition, states belonging to higher-lying structures above 2 MeV excitation energy are considerably lowered by the inclusion of triaxiality. A detailed analysis of triaxial shapes in the vibrational  $U(5)$ , rotational  $SU(3)$ , and  $\gamma$ -soft  $O(6)$  limits of the interacting boson model can be found in Ref. [11].

In the IBFM [8,9] calculation of negative-parity states in the odd- $Z$  neighbor  $^{135}_{59}\text{Pr}_{76}$  we have used the following values for the proton quasiparticle energies and occupation probabilities:  $\epsilon(\pi h_{11/2})=2.02$  MeV,  $\epsilon(\pi h_{9/2})=5.56$  MeV,  $\epsilon(\pi f_{7/2})=6.05$  MeV,  $v^2(\pi h_{11/2})=0.08$ ,  $v^2(\pi h_{9/2})=0.01$ ,  $v^2(\pi f_{7/2})=0.008$ . These values are obtained by a BCS calculation with the following single-particle energies: 0.18, 0.795, 2.248, 3.2, 3.41, 6.0, 6.5 (all values in MeV), for  $\pi g_{7/2}$ ,  $\pi d_{5/2}$ ,  $\pi h_{11/2}$ ,  $\pi d_{3/2}$ ,  $\pi s_{1/2}$ ,  $\pi h_{9/2}$ ,  $\pi f_{7/2}$ , respectively,

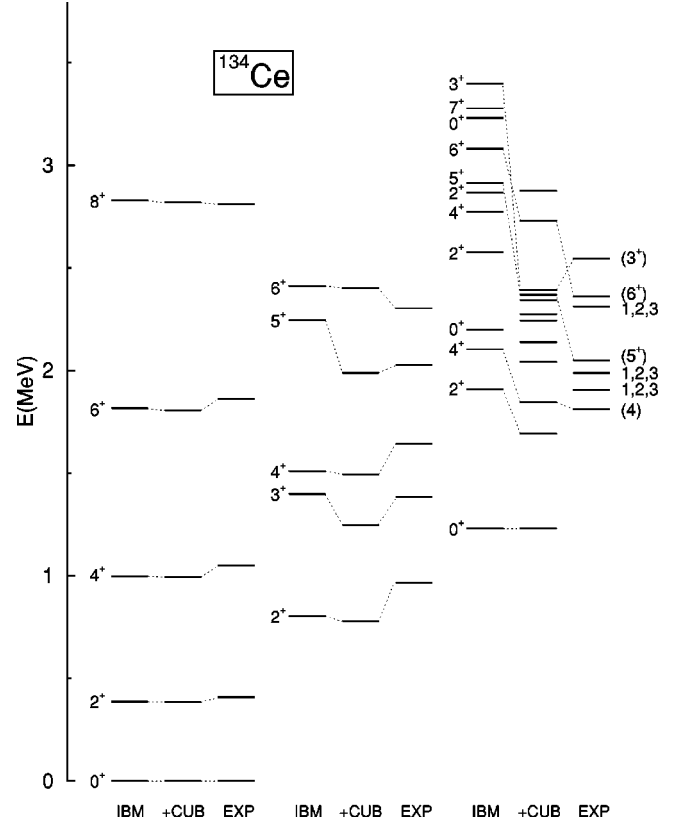


FIG. 1. IBM spectra of  $^{134}\text{Ce}$  shown in comparison with the experimental positive-parity levels (right columns). The levels in the left columns correspond to the IBM calculation with  $\Theta_3=0$  in the Hamiltonian (1), i.e., the term that induces triaxial deformation is not included. The nucleus is  $\gamma$  soft. The middle columns present the ground-state band, the  $\gamma$  band, and levels belonging to higher structures, calculated with  $\Theta_3=0.025$  MeV. The cubic term in the Hamiltonian induces a stable triaxial deformation.

and with the pairing strength  $G=23/A$  MeV. The single-proton energies in the  $Z=50-82$  shell are from Ref. [13]. The boson parameters are those of  $^{134}\text{Ce}$ , and the parameters of the boson-fermion interaction strengths read:  $A_0^\pi=0.09$ ,  $\Gamma_0^\pi=0.52$ ,  $\Lambda_0^\pi=0.5$  (all values in MeV). A very good agreement between the calculated negative-parity states and the experimental spectrum of  $^{135}\text{Pr}$  is obtained.

The neutron single-particle energies used in the calculation of  $^{133}_{58}\text{Ce}_{75}$  and  $^{134}_{59}\text{Pr}_{75}$  are from Ref. [14] for orbitals in the valence shell and from Ref. [15] for orbitals in the  $N=82-126$  shell. A BCS calculation with the pairing strength  $G=23/A$  MeV, and the neutron single-particle energies: 0, 0.4, 1.6, 2.0, 2.1, 7.0, 7.8, 8.5 (all values in MeV), for  $\nu d_{5/2}$ ,  $\nu g_{7/2}$ ,  $\nu s_{1/2}$ ,  $\nu d_{3/2}$ ,  $\nu h_{11/2}$ ,  $\nu f_{7/2}$ ,  $\nu p_{3/2}$ ,  $\nu h_{9/2}$ , respectively, is performed resulting in the quasiparticle energies and occupation probabilities of the neutron orbitals. In the IBFM calculation of the negative-parity states in  $^{133}\text{Ce}$  we have included only the lowest two quasiparticle states:  $\epsilon(\nu h_{11/2})=1.29$  MeV,  $\epsilon(\nu f_{7/2})=4.75$  MeV,  $v^2(\nu h_{11/2})=0.62$ ,  $v^2(\nu f_{7/2})=0.02$ . The best agreement with the  $^{133}\text{Ce}$  data is obtained for the choice of boson-fermion interaction strengths:  $A_0^\nu=0.12$ ,  $\Gamma_0^\nu=0.9$ ,  $\Lambda_0^\nu=1.4$  (all values in MeV).

In the final step of the calculation of positive-parity struc-

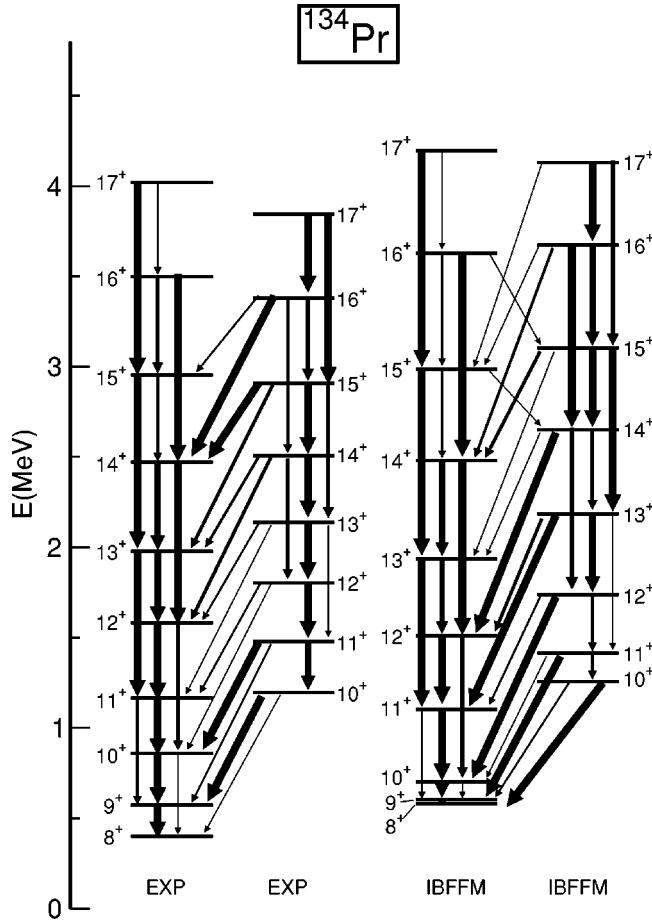


FIG. 2. Comparison of the experimental doublet of nearly degenerate positive-parity bands in  $^{134}\text{Pr}$  with the lowest two bands calculated in the IBFFM. The calculation includes the triaxial deformation of the core nucleus. The thickness of the arrows that denote transitions corresponds to the relative  $\gamma$  intensity in each branch.

tures in  $^{134}\text{Pr}$ , the residual odd proton–odd neutron interaction is taken in the form of a quadrupole–quadrupole interaction with the strength parameter  $V_2 = -0.4$  MeV. In addition, the agreement with the experimental spectrum is improved by fine tuning just a few parameters of the boson–fermion interactions:  $A_0^\pi = 0.05$ ,  $A_0^\nu = 0.1$ ,  $\Lambda_0^\nu = 1.6$  (all values in MeV).

With the inclusion of the three-body term in the boson Hamiltonian, the boson quadrupole operator appearing in the dynamical boson–fermion interaction and in the  $E2$  operator should also be extended to higher order. Following the analysis of Ref. [11], we have modified the standard boson quadrupole operator by including the additional term

$$\eta[(d^\dagger \tilde{d})_3 (d \tilde{d}^\dagger)_3]_2. \quad (2)$$

In the present calculation this term is included in the dynamical boson–fermion interaction and in the  $E2$  operator, with the strength parameter  $\eta = -0.46$  MeV.

In Fig. 2 the two lowest calculated positive-parity bands in  $^{134}\text{Pr}$  are shown in comparison with the experimental doublet bands. Both calculated bands are based on the  $\pi h_{11/2} \otimes \nu h_{11/2}$  configuration. We note that the calculation also pre-

dicts two states with angular momenta  $7^+$  and  $6^+$  at  $\approx 50$  keV below the state  $8_1^+$ . Such a small energy difference cannot be observed in experiment [16]. This situation is similar to the case of  $^{132}\text{Pr}$ , where the levels  $6^+$  and  $5^+$  are found below the band head  $7^+$ . In Ref. [17] it has been shown that these levels are predominantly based on positive-parity proton and neutron configurations. Accordingly we do not consider the states  $7_1^+$  and  $6_1^+$  as members of the yrast band in  $^{134}\text{Pr}$ . The admixture of components with positive-parity fermion configurations can also lower the energy of the  $8_1^+$  band head with respect to the  $9_1^+$  level. The comparison of the IBFFM results with the experimental levels is only possible up to angular momentum  $17^+$ . At higher excitation energies a four-quasiparticle band crosses the  $\pi h_{11/2} \otimes \nu h_{11/2}$  structure and becomes yrast. The admixture of four-quasiparticle components into the wave functions of the yrare band (not included in the present calculation) could probably account for the crossing between the two  $\pi h_{11/2} \otimes \nu h_{11/2}$  bands at lower spin, as compared with the prediction of the IBFFM calculation.

The calculated excitation energies of the two lowest  $\pi h_{11/2} \otimes \nu h_{11/2}$  bands are in good agreement with experimental data. In Fig. 2 we also display the calculated intensities for  $E2$  and  $M1$  transitions in comparison with the experimental values. The effective charges and gyromagnetic ratios are from Ref. [17], where they were used in the calculation of electromagnetic properties of  $^{132}\text{Pr}$ :  $e^\pi = 1.0$ ,  $e^\nu = 0.5$ ,  $g_l^\pi = 1$ ,  $g_s^\pi = 0.5$ ,  $g_s^{\pi, \text{free}} = 2.793$ ,  $g_l^\nu = 0$ ,  $g_s^\nu = 0.5$ ,  $g_s^{\nu, \text{free}} = -1.913$ ,  $g_R = Z/A = 0.44$ . The boson charge is  $e^{\text{vib}} = 2.0$ . The  $\gamma$  intensities in Fig. 2 show a good agreement between theory and experiment, especially for transitions within the bands. The calculation predicts somewhat stronger interband transitions in the low-energy part of the spectrum. This is a consequence of the IBFFM wave functions that in the lower part of the yrare band probably overestimate the contribution of  $\gamma$ -band components. Although such structure does not have a strong  $M1$  decay to the yrast band, a closer inspection of the transition probabilities shows that the interband  $M1$  transitions are too small only for the two lowest yrare states. The main disagreement comes from  $E2$  transitions that are stronger than the experimentally observed. The interband  $E2$  transitions are small when compared to those within the band, but IBFFM (as a collective model) however overestimates their values.

The most interesting new result is the model prediction for the collective structure of the wave functions of the two lowest  $\pi h_{11/2} \otimes \nu h_{11/2}$  bands. The yrast band is basically built on the ground-state band of the even–even core. With increasing angular momentum the admixture of the  $\gamma$  band of the core becomes more pronounced. The structure of the second-yrare band, however, is that of the odd proton and odd neutron coupled to the  $\gamma$  band of the core, especially in the lower part of the band. With increasing angular momentum both ground-state band and  $\gamma$ -band components contribute to the wave functions of the yrare band in  $^{134}\text{Pr}$ . In the region of band crossing, in particular, the wave functions of the yrare band contain sizeable components of the higher-lying core structures (see the right column in Fig. 1). The IBFFM prediction, therefore, is that the two lowest  $\pi h_{11/2} \otimes \nu h_{11/2}$  bands in  $^{134}\text{Pr}$  are built, in leading order, on the ground-state band and the  $\gamma$  band of the core nucleus, respectively. Their wave functions closely follow the triaxial struc-

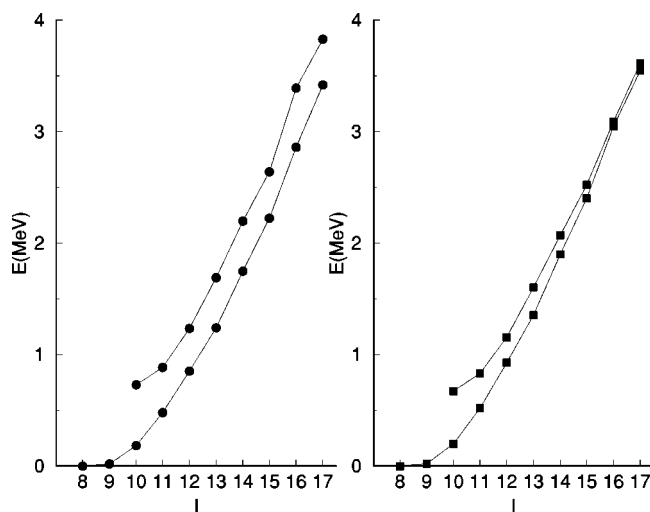


FIG. 3. The yrast and yrare  $\pi h_{11/2} \otimes \nu h_{11/2}$  bands in  $^{134}\text{Pr}$  calculated in the IBFFM for the  $^{134}\text{Ce}$  core without triaxiality (left panel,  $\Theta_3=0$ ), and with stable triaxial deformation (right panel,  $\Theta_3=0.03$  MeV).

ture of the core nucleus. As the IBFFM calculations are performed in the laboratory frame, they cannot determine the alignment of the odd particles along the body fixed axes. The present analysis, focused on the collective structure of the doublet bands, indicates that the  $\gamma$  degree of freedom plays an important role in their formation.

The effect of the triaxial deformation is illustrated in Fig. 3, where we display the yrast and yrare  $\pi h_{11/2} \otimes \nu h_{11/2}$  bands in  $^{134}\text{Pr}$  calculated in the IBFFM for the  $^{134}\text{Ce}$  core without triaxiality (left panel,  $\Theta_3=0$ ), and with stable triaxial deformation (right panel,  $\Theta_3=0.03$  MeV). For  $\Theta_3=0$  the core is  $\gamma$  soft and the two bands do not cross or become degenerate. Rather, an almost constant energy spacing  $\approx 400$  keV between the two bands is predicted. For a stable triaxial defor-

mation ( $\Theta_3=0.03$  MeV) the energy difference between the yrast and yrare bands gradually decreases, and between angular momenta  $16^+$  and  $17^+$  the two bands cross. Except for the exact position of the band crossing (which can be also affected by four-quasiparticle configurations not included in the model space), the “energy vs spin” diagram in the right panel of Fig. 3 is in excellent agreement with the experimentally observed evolution of the two lowest positive-parity bands in  $^{134}\text{Pr}$ . The results shown in Fig. 3 are also in agreement with the conclusions of Ref. [3], where it has been suggested that in the odd-odd  $N=75$  nuclei other than  $^{134}\text{Pr}$  the triaxial core deformation is not stable, rather it is  $\gamma$ -soft, resulting in the two lowest  $\pi h_{11/2} \otimes \nu h_{11/2}$  bands being almost parallel in the  $E$  vs  $I$  plot, with the energy spacing of  $\approx 0.3$  MeV. In  $^{134}\text{Pr}$ , on the other hand, the stable triaxial deformation causes the two lowest positive-parity bands to become almost degenerate.

In conclusion, the structure of the two lowest and almost degenerate positive-parity bands in  $^{134}\text{Pr}$  has been investigated in the framework of the interacting boson fermion-fermion model. A very detailed analysis, which also includes the calculation of the spectra of the even-even and odd-even neighbors, has demonstrated that stable triaxial deformation gives rise to the experimentally observed crossing between the yrast and yrare bands built on the  $\pi h_{11/2} \otimes \nu h_{11/2}$  configuration. A constant energy spacing between the two lowest positive-parity bands is predicted in other odd-odd  $N=75$  nuclei with  $\gamma$ -soft potential energy surfaces. The analysis of the wave functions and transition intensities has shown that the collective structure of the yrast band in  $^{134}\text{Pr}$  is basically built on the ground-state band of the triaxial core, whereas the collective structure of the yrare band is predominantly based on the  $\gamma$  band of the core. The mixing between the two bands increases with increasing angular momentum, and the region of band crossing is characterized by sizeable admixtures of higher-lying collective structures.

- [1] S. Frauendorf and J. Meng, Nucl. Phys. **A617**, 131 (1997).  
 [2] V. I. Dimitrov, S. Frauendorf, and F. Dönau, Phys. Rev. Lett. **84**, 5732 (2000).  
 [3] K. Starosta *et al.*, Phys. Rev. Lett. **86**, 971 (2001).  
 [4] V. Paar, in *Capture Gamma-Ray Spectroscopy and Related Topics-1984*, edited by S. Raman, AIP Conf. Proc. No. 125 (AIP, New York, 1985), p. 70; S. Brant, V. Paar, and D. Vretenar, Z. Phys. A **319**, 355 (1984); V. Paar, D. K. Sunko, and D. Vretenar, Z. Phys. A **327**, 291 (1987).  
 [5] S. Brant and V. Paar, Z. Phys. A **329**, 151 (1988).  
 [6] F. Iachello and A. Arima, *The Interacting Boson Model* (Cambridge University Press, Cambridge, 1987).  
 [7] A. Arima and F. Iachello, Phys. Rev. Lett. **35**, 157 (1975); Ann. Phys. (N.Y.) **99**, 233 (1976); **111**, 201 (1978); **123**, 468 (1979).  
 [8] F. Iachello and O. Scholten, Phys. Rev. Lett. **43**, 679 (1979).  
 [9] F. Iachello and P. Van Isacker, *The Interacting Boson Fermion Model* (Cambridge University Press, Cambridge, 1991).  
 [10] Y. Tokunaga, H. Seyfarth, O. W. B. Schult, S. Brant, V. Paar, D. Vretenar, H. G. Börner, G. Barreau, H. Faust, Ch. Hofmeyr, K. Schreckenbach, and R. A. Meyer, Nucl. Phys. **A430**, 269 (1984).  
 [11] K. Heyde, P. Van Isacker, M. Waroquier, and J. Moreau, Phys. Rev. C **29**, 1420 (1984).  
 [12] R. F. Casten, P. von Brentano, K. Heyde, P. Van Isacker, and J. Jolie, Nucl. Phys. **A439**, 289 (1985).  
 [13] L. S. Kisslinger and R. A. Sorensen, Rev. Mod. Phys. **35**, 853 (1963).  
 [14] Gh. Cata-Danil, D. Bucurescu, A. Gizon, and J. Gizon, J. Phys. G **20**, 1051 (1994).  
 [15] B. S. Reehal and R. A. Sorensen, Phys. Rev. C **2**, 819 (1970).  
 [16] C. M. Petrache, D. Bazzacco, S. Lunardi, C. Rossi Alvarez, G. de Angelis, M. De Poli, D. Bucurescu, C. A. Ur, P. B. Semmes, and R. Wyss, Nucl. Phys. **A597**, 106 (1996).  
 [17] C. M. Petrache, S. Brant, D. Bazzacco, G. Falconi, E. Farnea, S. Lunardi, V. Paar, Zs. Podolyák, R. Venturelli, and D. Vretenar, Nucl. Phys. **A635**, 361 (1998).